

# Low-Temperature Emission Spectra of 9-Alkylanthracene Esters: Dimer Photodecomposition and Monomer Pair Interactions in Polymer Hosts

Kimberly Salt and Gary W. Scott\*

Department of Chemistry, University of California, Riverside, Riverside, California 92521

Received: April 11, 1994; In Final Form: July 12, 1994<sup>⊗</sup>

Effects due to variation in the alkyl chain length of photodimers of 9-alkylanthracene esters on their photodecomposition efficiencies at 12 K and, by implication, the photoproduct migration as a function of temperature within polymer hosts are investigated. It is shown that dimers with longer alkyl chains have a lower photodecomposition efficiency. The extent of photoproduct migration within the polymer following photodecomposition was also studied as a function of alkyl chain length. This migration and its modulation of the interaction between the separating monomers is shown to affect the emission spectrum. Thus, monomer migration was studied in temperature cycling experiments. It was also found, for the polymer hosts investigated—poly(methyl methacrylate), poly(vinyl chloride), and polystyrene—that these properties are host dependent. This result is probably due to the void space differences that exist among these polymers.

## 1. Introduction

Over a century ago,<sup>1</sup> it was discovered that polycyclic aromatic hydrocarbons such as anthracene form thermally stable photoproducts, later identified as photodimers. About 30 years ago it was realized that these dimers can be cleaved photochemically to the original monomers by irradiation with light of a suitable wavelength.<sup>2</sup> Cleaving these dimers results in an extended aromatic system that was disrupted upon dimer formation. This photochemical decomposition results in a red shift of the relatively strong, lowest energy  $\pi$ - $\pi^*$  absorption band. This phenomenon has prompted the investigation of these photodimers as potential candidates for use in photochromic materials which are thermally stable in both states but photo-reversible.<sup>3</sup>

The oldest known photodimer of this type, first synthesized photochemically in 1866, is dianthracene.<sup>1</sup> Our group has recently reported the low temperature spectroscopy and photochemistry of dianthracene.<sup>4</sup> Other derivatives of anthracene have also been dimerized but not studied as extensively as has dianthracene. One such class of derivatives is the 9-alkyl esters of anthracene (9-anthroate esters). It was previously shown that the length of the alkyl side chain in the ester has a measurable influence on the efficiency of the dimerization of these molecules in room temperature solution.<sup>5</sup> Of additional interest, particularly if these materials are to be used as the basis of photochromic materials, is what influence, if any, the alkyl chain length has on the dimer photostability. In the present study, we investigate the effects of the alkyl chain length of five different 9-anthroate esters on the photodecomposition of the respective photodimers and the extent of molecular migration subsequent to their photodecomposition within polymer host matrices. The structures of these photodimers are shown in Figure 1.

## 2. Experimental Methods

9-Alkyl esters of anthracene (methyl, ethyl, 1-propyl, *n*-butyl, and 1-pentyl) were synthesized from 9-anthric acid (Aldrich) using a variation of the procedure outlined by Parish and Stock.<sup>6</sup> 9-Anthric acid (1 g) was suspended in 15 mL of methylene chloride, and then 2.5 mL of trifluoroacetic anhydride was slowly added. The mixture was stirred until the acid dissolved,

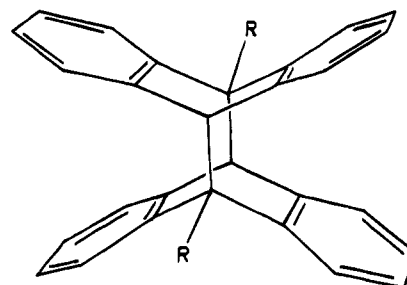


**Figure 1.** Photodimers of 9-anthroate ester. The photodimers investigated had R =  $-\text{C}(=\text{O})-\text{O}-\text{CH}_3$ ,  $-\text{C}(=\text{O})-\text{O}-\text{CH}_2\text{CH}_3$ ,  $-\text{C}(=\text{O})-\text{O}-\text{CH}_2\text{CH}_2\text{CH}_3$ ,  $-\text{C}(=\text{O})-\text{O}-\text{CH}_2\text{CH}_2\text{CH}_2\text{CH}_3$ , and  $-\text{C}(=\text{O})-\text{O}-\text{CH}_2\text{CH}_2\text{CH}_2\text{CH}_2\text{CH}_3$ .

and then 2.5 mL of the appropriate alcohol was added. The reaction mixture was stirred for 2 h to ensure completion of the reaction. The solvent was then evaporated, and the resulting solid was recrystallized from ethyl acetate. Product yields were somewhat lower than those reported by Parish and Stock.<sup>6</sup> Confirmation of product structure was done by taking IR and NMR spectra and by confirming melting points.

Photodimers were prepared by irradiating saturated toluene solutions of the appropriate monomer with visible/near UV light ( $\lambda > 345$  nm) filtered from a high-pressure mercury lamp. The dimer was isolated by vacuum filtration and then rinsed several times with ethyl acetate to remove any unreacted monomer. UV-visible absorption spectra and melting points were consistent with those reported in the literature.<sup>5</sup>

Each photodimer was blended into three different polymer matrices—poly(methylmethacrylate), poly(vinyl chloride), and polystyrene. High molecular weight poly(methyl methacrylate) (PMMA, MW = 30 000, Aldrich) and low molecular weight poly(vinyl chloride) (PVC, Aldrich) were purified by repeated reprecipitation and Soxhlet extraction as previously described.<sup>7</sup> Polystyrene (PS, MW = 250 000, Aldrich) was used without further purification. Polymer films incorporating the various photodimers were prepared by casting from dichloromethane solutions. Film thicknesses were typically 0.4 mm with absorbances of  $\approx 0.5$  at the wavelength of the origin absorption band (282 nm) of the benzene chromophore  $S_0 \rightarrow S_1$  transition for the photodimer.

Fluorescence spectra were obtained with a SPEX Fluorolog 212 spectrofluorimeter equipped with a 450 W xenon lamp

<sup>⊗</sup> Abstract published in *Advance ACS Abstracts*, September 1, 1994.

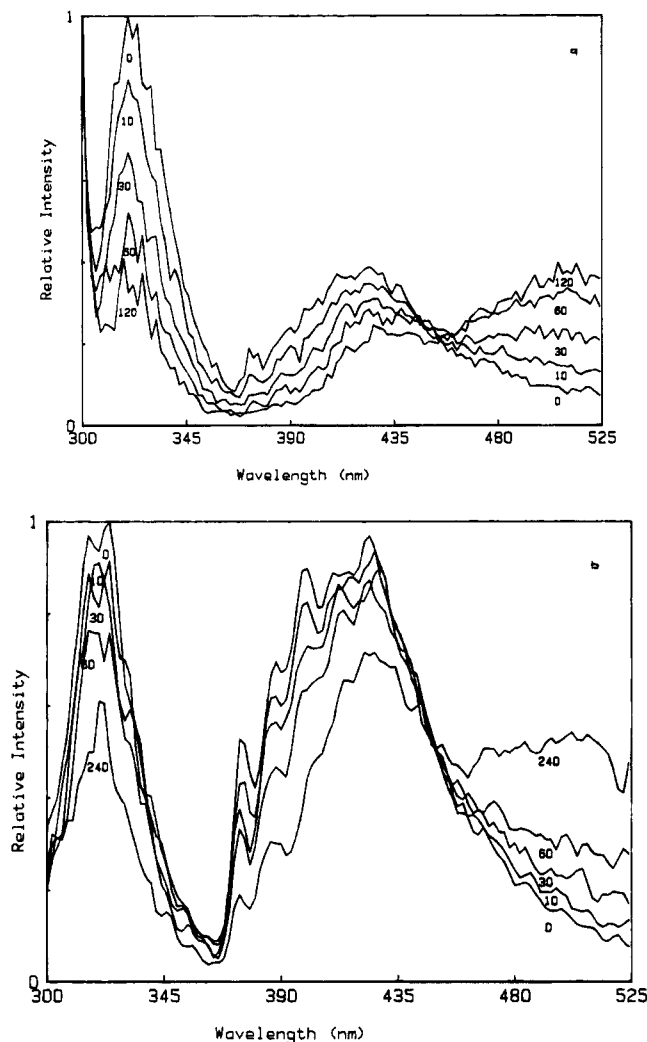


**Figure 2.** (a) Emission spectra of 9-ethyl anthroate dimer in PMMA at 12 K vs irradiation time at 275 nm. Spectra were obtained at 0, 10, 30, 60, and 120 min of irradiation as indicated. (b) Emission spectra of 9-pentyl anthroate dimer in PMMA at 12 K vs irradiation time at 275 nm. Spectra were obtained at 0, 10, 30, 60, and 240 min of irradiation as indicated.

excitation source, two  $1/4$ -m double monochromators with 1.5 nm/mm inverse linear dispersion, and a cooled photomultiplier tube with photon-counting electronics. The fluorescence signal was ratioed to the excitation photon flux using a quantum counter. Photodecomposition of the polymer samples was carried out by irradiating them at the photolysis wavelength using the spectrofluorimeter excitation source with the monochromator slits set at a bandpass of 0.36 nm. In these experiments, the spectra were recorded at 2-nm intervals with only a 1-s integration time in order to minimize photodecomposition during the time for recording a single spectrum ( $\sim 3$  min).

Spectra at low temperature (12 K) were obtained by cooling the sample in a closed-cycle helium refrigerator with optical access.

### 3. Results

Figure 2a,b shows typical emission spectra obtained from a sample of 9-ethyl and 9-pentyl anthroate photodimers, respectively, in PMMA at 12 K as a function of irradiation time at 275 nm. (These spectra appear somewhat noisy due to the need to record them rapidly as explained above.) In these spectra, the emission peaking at  $\sim 320$  nm is assigned to photodimer

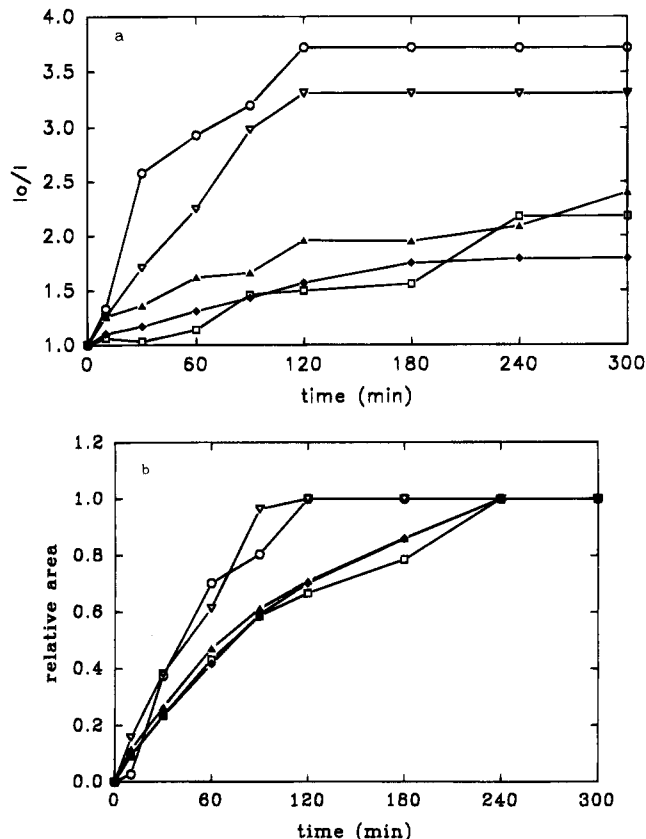


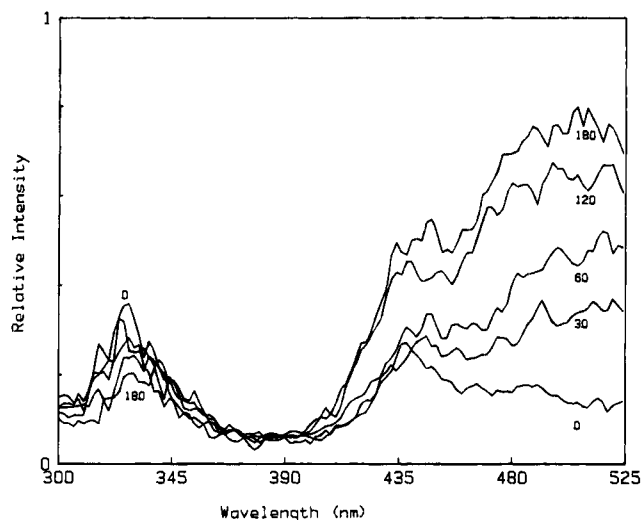
**Figure 3.** (a) Integrated photodimer fluorescence (300–365 nm) at the indicated irradiation times divided into the zero time value. (b) Integrated sandwich dimer fluorescence (455–515 nm) at the indicated irradiation times normalized to the long time value. Irradiations were at 275 nm, all in PMMA at 12 K ( $\circ$  = methyl;  $\nabla$  = ethyl;  $\square$  = propyl;  $\blacktriangle$  = butyl; and  $\blacklozenge$  = pentyl).

fluorescence, that at  $\sim 425$  nm to its phosphorescence, and that at lower energies to photoproduct fluorescence. For all five of the 9-alkyl anthroate photodimers in PMMA samples, measurable changes in the emission spectra were seen after 10 min of irradiation. Figure 3a shows the time evolution of the photodimer fluorescence for all five of the molecules studied in PMMA by plotting  $I_0/I$ , where  $I_0$  is wavelength-integrated fluorescence intensity at zero time and  $I$  is the same at time  $t$ . Figure 3b shows the buildup in the relative, wavelength-integrated product fluorescence as a function of time. All intensities were normalized to the long-time integrated fluorescence.

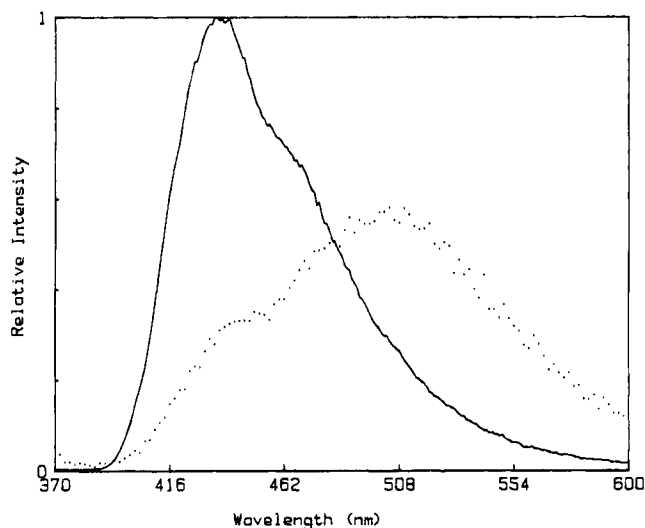
Figure 4 shows emission spectra of 9-ethyl anthroate photodimer in PVC at 12 K as a function of the irradiation time at 275 nm. For all of the photodimers in a PVC film photodecomposition takes considerably longer than in a PMMA film, with the longer alkyl chain esters taking the longest time.

Figure 5 compares the emission spectrum of an authentic sample of 9-ethyl anthroate monomer in PMMA at 12 K with that of the 9-ethyl anthroate photodimer decomposition product under the same conditions.

Figure 6a,b shows the results of temperature cycling on the emission spectra of the photoproducts following photolysis of PMMA samples of the 9-ethyl and 9-pentyl anthroate photodimers, respectively. Prior to the cycling, photolysis at 275 nm was carried out for 1 h. After this period, the photoproduct emission spectrum was obtained from the sample at 12 K by exciting at 340 nm. The sample was then warmed to and held at 50 K in the dark for 1 h, recooled to 12 K, and the photoproduct emission spectrum retaken in the same manner.



**Figure 4.** Emission spectra of 9-ethyl anthroate dimer in PVC at 12 K vs irradiation time at 275 nm. Spectra were obtained at 0, 30, 60, 120, and 180 min of irradiation as indicated.



**Figure 5.** Emission spectra of 9-ethyl anthroate monomer (—) and the broken dimer product of 9-ethyl anthroate (···) in PMMA at 12 K. Excitation wavelength was at 340 nm in both cases.

This procedure was repeated for sequentially increasing upper temperatures of the cycle. Similar temperature cycling results on photolyzed dimers in a PVC host are shown for 9-methyl anthroate and the 9-ethyl anthroate in Figure 7a,b, respectively. Figure 8 illustrates similar results for the photolyzed 9-methyl anthroate dimer product emission in a polystyrene host. The relative fluorescence intensities at 410 nm as a function of the upper temperature of the cycle for all five 9-alkyl anthroates (Figure 1) in PMMA, in PS, and in PVC, are shown in Figure 9a–c, respectively.

#### 4. Discussion

When a 9-alkyl anthroate dimerizes, the dimer forms by bridging the 9 and 10 carbons of the two anthracenes, respectively, with the substituents in a head to tail orientation as shown in Figure 1. Thus, the dimer consists of essentially four benzene chromophores linked together by a network of carbon–carbon single bonds.<sup>4</sup>

When the dimer is photochemically cleaved, the bonds between the 9 and 10' and the 9' and 10 carbon atoms are broken, reestablishing the aromaticity of the central rings in the two anthracene monomers. When dimer cleavage occurs at low

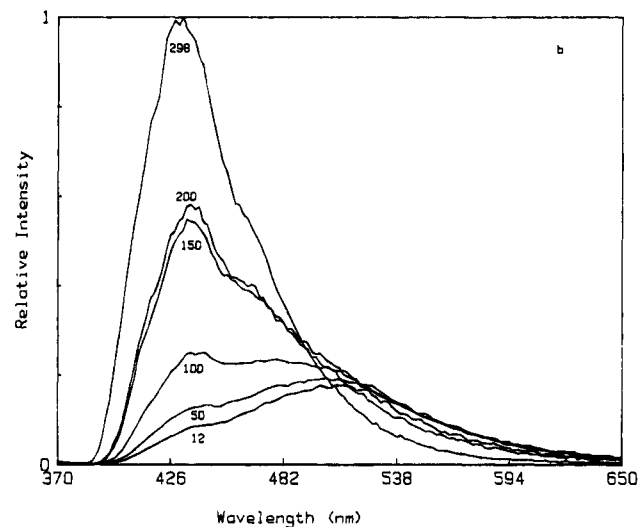
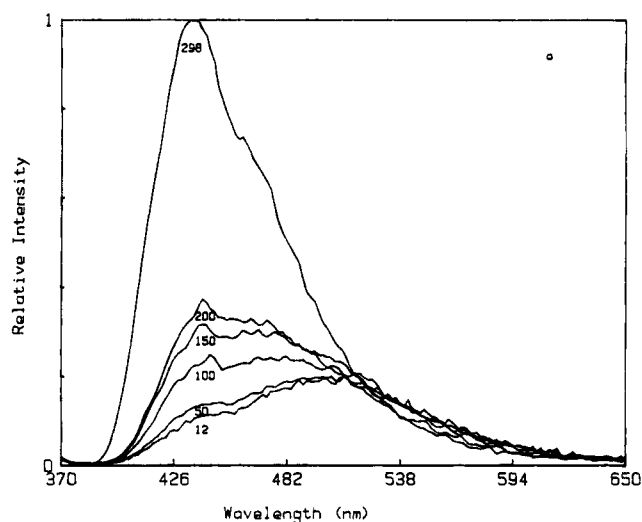


**Figure 6.** Emission spectra of broken dimers in PMMA at 12 K as a function of temperature cycling. Excitation is at 340 nm. All spectra were obtained at 12 K after cycling up to 12, 50, 100, 150, 200, and 298 K: (a) 9-ethyl anthroate; (b) 9-butyl anthroate.

temperature, the surrounding rigid host matrix hinders separation of the monomer halves, constraining them to an interacting configuration of the two monomers which has been termed in the literature a sandwich or broken dimer.<sup>2,10</sup> This sandwich dimer exhibits a red-shifted excimer-like emission upon excitation into the monomer absorption band.<sup>2,10</sup>

As seen in Figure 2a, the fluorescence and phosphorescence intensities of the 9-ethyl anthroate dimer decrease with irradiation time, indicating that the dimer is being broken. Simultaneously, a new emission band on the red edge of the spectrum, assigned to the sandwich dimer, increases in intensity. The isoemissive point at  $\sim 455$  nm indicates that only the dimer and the sandwich dimer are being observed. After  $\approx 120$  min of irradiation, the emission spectrum reaches a steady state, and no further changes are observed at subsequent times.

Similar results (Figure 2b) were observed for PMMA samples of the 9-pentyl anthroate dimer at 12 K. In this case, however, the photodecomposition, as monitored by the product emission spectrum, does not reach a steady state until  $\approx 240$  min of irradiation time. In a previous study<sup>13</sup> of the 9-pentyl anthroate dimer in PMMA the estimated quantum yield for dimer breaking was given as 0.3. However, this earlier study was performed at room temperature and therefore is not directly comparable with the present study of dimer photodecomposition at 12 K. As indicated above, for all of the 9-alkyl anthroate dimer

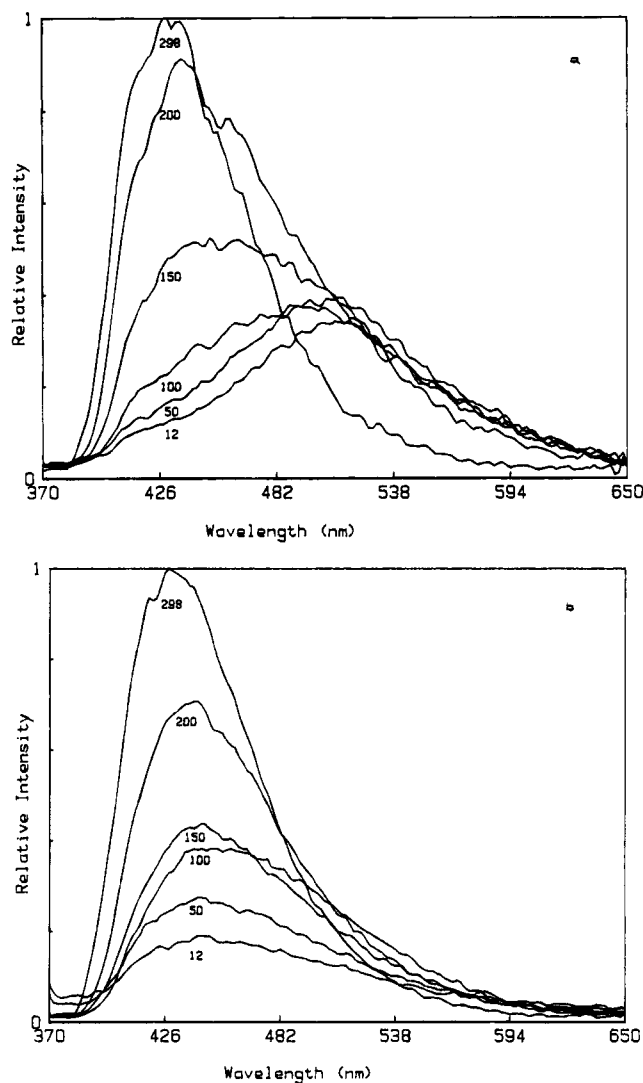


**Figure 7.** (a) Emission spectra of 9-methyl anthroate broken dimer in PVC at 12 K as a function of temperature cycling. Excitation was at 340 nm. All spectra were obtained at 12 K after cycling up to 12, 50, 100, 150, 200, and 298 K. (b) Emission spectra of 9-ethyl anthroate broken dimer in PVC at 12 K as a function of temperature cycling. In both cases excitation was at 340 nm, and spectra were obtained after cycling to 12, 50, 100, 150, 200, and 298 K.

samples in the PMMA matrix, significant changes in the emission spectra are seen after 10 min of irradiation at 275 nm, signaling the onset of dimer photodecomposition. As shown in Figures 3a,b, a longer irradiation time is required to reach a steady-state emission spectrum for longer alkyl chain length esters, implying a lower efficiency for photodecomposition. Thus, longer alkyl chains tend to stabilize the dimer with respect to photodecomposition, probably due to a more rigid coupling between the host matrix and the ester's alkyl chain.

Photodimers incorporated within a PVC matrix show a somewhat different behavior (see Figure 4). The 9-methyl and 9-ethyl anthroate dimers do not exhibit much of a change in their emission spectra until  $\approx 30$  min of irradiation, indicating a lower efficiency of photodecomposition at 275 nm in the PVC matrix than in the PMMA matrix at 12 K. In addition, both of these compounds take longer to reach a steady state of photodecomposition which occurs after  $\approx 180$  min of irradiation. For the 9-propyl, 9-butyl, and 9-pentyl anthroate dimers in PVC, the first detectable changes in the emission spectra occur only after  $\approx 60$  min of irradiation at 275 nm. The 9-propyl anthroate dimer spectrum reaches a steady state after  $\approx 240$  min, that of the 9-butyl anthroate dimer after  $\approx 300$  min, while the 9-pentyl

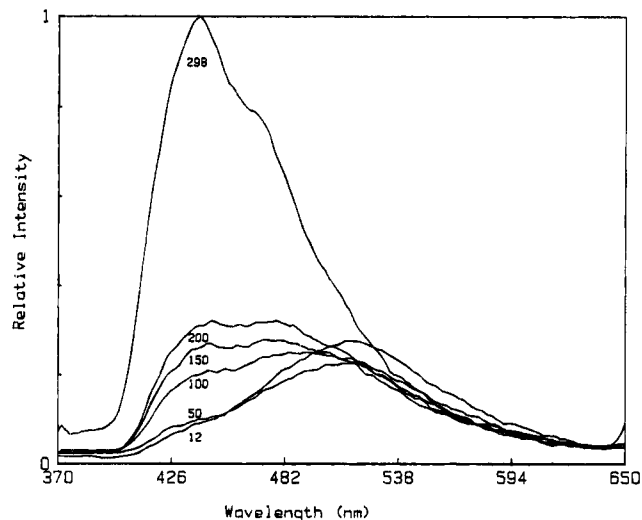


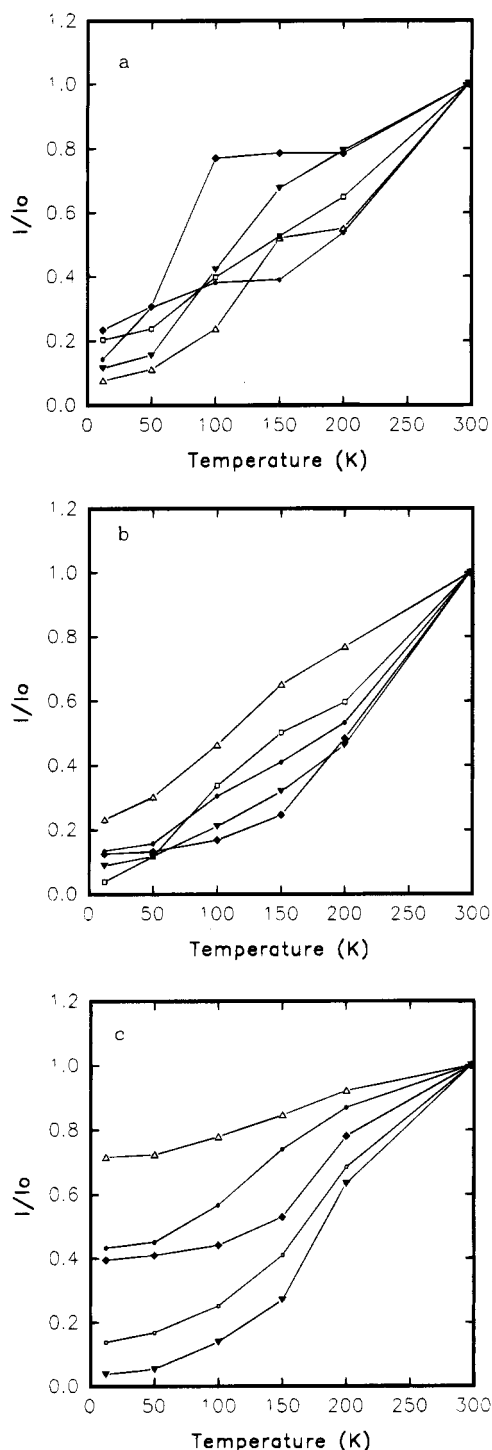
**Figure 8.** Emission spectra of 9-methyl anthroate broken dimer in PS at 12 K as a function of temperature cycling. Excitation is at 340 nm. All spectra were obtained at 12 K after cycling up to 12, 50, 100, 150, 200, and 298 K.

anthroate dimer shows very little photodecomposition even after  $\approx 480$  min of irradiation in PVC. Thus, there is a lower photodecomposition efficiency for all photodimers in the PVC matrix than in the PMMA host. One possible cause of this behavior could be a smaller sized host cavity for the guest dimers in the PVC matrix than in the PMMA host. Another possibility is the presence of an external heavy atom effect on the dimers by the PVC matrix. (Certainly dimers in the PVC matrix exhibit more phosphorescence than they do in the PMMA matrix, a result most likely due to an external heavy atom effect. Such an increased phosphorescence intensity simply means that the triplet lifetime of the dimer is shorter in the PVC matrix, allowing less opportunity for excitation of an upper triplet level such as may be required for photodecomposition in analogy with  $A_2$  at low temperature.<sup>4</sup>) We tend to favor the first possible explanation since PVC has a lower glass transition temperature (354 K) than PMMA (378 K) and hence is expected to have the smallest void space of the three polymer hosts studied.

From the comparison of monomer and photoproduct emission spectra in Figure 5, it is clear that the energy distribution of the photoproduct spectrum differs drastically from that of the monomer. This indicates that the dimer does not directly break into two *noninteracting* monomer units but that the monomer units remain in close vicinity to each other, resulting in perturbed dimer states for the interacting dimer pair.

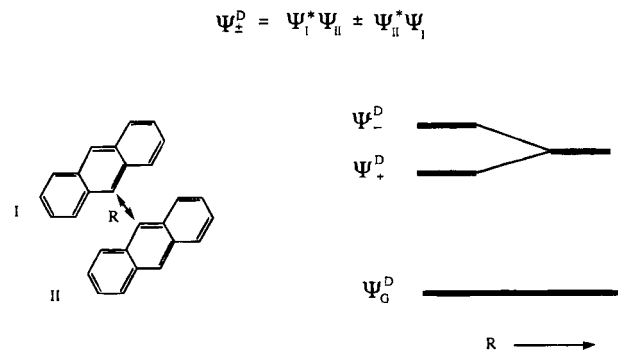
As the sample temperature is increased (Figure 6), there is a gradual blue shift in the photoproduct emission spectrum. This shift can be attributed to migration of the guest as well as motion of the host that should be thermally activated in the host matrix. At a low temperature (12 K), the photochemically formed anthroate sandwich dimers are constrained by a rigid host cavity. Although the size and shape of this cavity are host dependent, nevertheless the two anthroate molecules can separate only by a restricted amount before encountering a repulsive surface due to the surrounding polymer. The change in the observed emission spectrum upon temperature cycling to a higher temperature and back to 12 K indicates that at the higher temperature the two anthroate molecules migrate away from the repulsive sandwich dimer configuration. Eventually, they separate far enough from one another so that they may act as two separate, noninteracting monomer units.<sup>4,10</sup>

Figure 9 plots the relative fluorescence intensity at 410 nm of 9-alkyl anthroates at 12 K in PMMA, PS, and PVC as a result of excitation at 340 nm and as a function of the maximum



**Figure 9.** Relative fluorescence intensity at 410 nm and 12 K while exciting at 340 nm as a function of the temperature cycle maximum. Values are normalized to the 300 K intensity ( $I_0$ ): (a) PMMA host, (b) PS host, and (c) PVC host. In each case the data are designated as 9-methyl anthroate (●), 9-ethyl anthroate (□), 9-propyl anthroate (◆), 9-butyl anthroate (△), and 9-pentyl anthroate (▼).

in the temperature cycle. The monitoring fluorescence wavelength (410 nm) provides a measure of predominantly noninteracting monomer fluorescence and hence provides a gauge of the proportion of anthroate monomers which have "escaped" from a sandwich dimer configuration. This type of temperature cycling data provides information on the distribution of barriers to monomer migration in these disordered systems. Figure 9 indicates that this distribution is not a monotonically decreasing function of barrier height. Also the barrier distribution is somewhat different in PVC than in PMMA. This type of



**Figure 10.** Schematic depiction of how broken dimer separation (left) leads to shifts in the emission spectra due to the energy level diagram (right).

experiment provides complementary information to spectral hole-filling experiments such as those reported for organic polymers and glasses by Friedrich and co-workers.<sup>11-16</sup> Although our technique provides less detail and perhaps more ambiguity, we can monitor the barrier distribution to higher energies (i.e., by observing changes due to higher cycling temperatures) than can be monitored in such hole-filling experiments.

Figure 10 schematically depicts the separation of the broken dimer, showing the changes which occur in the electronic energy level diagram during this separation.<sup>17</sup> Each monomer wavefunction ( $\psi_I$  and  $\psi_{II}$ ) describes the state of molecule I or II. When the distance between the two monomers is short, as in the initially formed broken dimer at low temperature, the  $\pi$  orbitals strongly interact with one another, forming a dimer system with two excited electronic state wave functions which split in energy about that of an isolated monomer. As the monomers separate, the interaction between them decreases with the state functions reducing to those of isolated monomers. Thus, a blue shift occurs in the emission spectrum with the increasing temperature maximum of the experimental temperature cycle.

From the data obtained, it appears that for the 9-methyl and 9-ethyl anthroate dimer samples, the PMMA matrix allows most if not all of the sandwich dimers to reach a noninteracting isolated monomer separation at 298 K. However, for the 9-propyl, 9-butyl, and 9-pentyl anthroates, most molecules reach this separation at a lower temperature of  $\approx 150$  K. Thus, it appears that the longer chain esters may be incorporated into larger cavities within the polymer matrix; thereby allowing thermally activated motion of the guest molecules to occur at lower temperatures.

In the PVC matrix, the 9-methyl and 9-pentyl photoproduct emission is initially centered at  $\approx 512$  nm. When the samples are cycled to 150 K, a large blue shift occurs in the spectrum; although, the majority of the molecules do not appear to reach the monomer separation until they are cycled up to 298 K. However, the behaviors of the 9-ethyl, 9-propyl, and 9-butyl anthroate dimers in this matrix are quite different as shown in Figure 7. First, the photoproduct emission is not as broad or as red-shifted as in the cases of the methyl and pentyl dimers. That is, the initial photoproduct emission peaks are centered at  $\approx 450$  nm for the 9-ethyl, 9-propyl, and 9-butyl anthroates, and these spectra do not differ greatly from the monomer emission spectra. This observation may indicate that the solvent cage in which these three molecules are held may allow them to move rather freely even at very low temperatures. In the case of the pentyl dimer, one may speculate that the longer alkyl chain may tether the dimer to the polymer matrix thus precluding more extensive motion of the broken dimer at low temperatures. For the methyl dimer, one may deduce that a shorter chain length

allows the polymer to constrain this dimer in a smaller cavity thereby restricting its motion after photodecomposition at low temperatures.

Figure 8 shows that the initial photoproduct emission of the 9-methyl anthroate broken dimer is broad and centered at 512 nm in the polystyrene matrix. As the temperature is cycled to progressively higher temperatures, no emission blue shift is seen until the temperature is cycled to above 100 K. After cycling up to this temperature, the spectrum is even broader than the original 12 K spectrum, and it does not resemble the monomer emission. After cycling the sample temperature to 298 K, the emission spectrum resembles that of the monomer. This same temperature cycling effect is also seen in all five dimer samples in polystyrene. The broadening of the 12 K emission after cycling to 100 K is probably due to an increase in the cavity size inhomogeneity, allowing a greater range of  $R$  distances (Figure 10) between monomer units. Upon further warming, the increased thermal energy allows additional increases in  $R$  throughout the sample so that significant dimer interactions no longer occur in any cavity.

Thus, it has been observed that the alkyl chain length in 9-alkyl anthroates and the host polymer structure affects the efficiency of the respective dimer's photodecomposition. Hence, the interaction between the guest dimers and the host matrix plays a significant role in the photochemistry of these systems. It is concluded that chain length effects on the photodecomposition efficiencies of the 9-alkyl anthroate dimers are likely due to the interactions between the host matrix and the alkyl chain of the ester. The interaction generally increases as the chain length grows thereby leading to a reduced efficiency of photodecomposition. In addition, the matrix also influences the extent of monomer separation following dimer photodecompo-

sition. Thus the length of the ester's alkyl chain of the ester in combination with the size of the polymer matrix cavity influences the temperature at which the sandwich dimer is free to separate into two individual noninteracting monomers.

**Acknowledgment.** This research was supported by funds from the Committee on Research, University of California, Riverside. Additional support was provided by the INCOR grant program administered through the Center for Nonlinear Studies at Los Alamos National Laboratory.

## References and Notes

- (1) Frizsche, J. *J. Prakt. Chem.* **1866**, 101, 337.
- (2) Chandross, E. A. *J. Chem. Phys.* **1965**, 43, 4175.
- (3) Tomlinson, W. J.; Chandross, E. A.; Fork, R. L.; Pryde, C. A.; Lamola, A. A. *Appl. Opt.* **1972**, 11, 533.
- (4) Iannone, M. A.; Scott, G. W. *Mol. Cryst. Liq. Cryst.* **1992**, 211, 375.
- (5) Shon, R. S.; Cowan, D. O.; Schmiegel, W. W. *J. Phys. Chem.* **1975**, 79, 2087.
- (6) Parish, R. C.; Stock, L. M. *J. Org. Chem.* **1965**, 30, 927.
- (7) Iannone, M. A.; Scott, G. W.; Brinza, D.; Coulter, D. R. *J. Chem. Phys.* **1986**, 85, 863.
- (8) Chandross, E. A.; Ferguson, J.; McCrae, E. G. *J. Chem. Phys.* **1966**, 45, 3546.
- (9) Ferguson, J.; Mau, A. W.-H.; Morris, J. M. *Aust. J. Chem.* **1973**, 26, 91.
- (10) Ferguson, J.; Mau, A. W.-H. *Mol. Phys.* **1974**, 27, 377.
- (11) Köhler, W.; Meiler, J.; Friedrich, J. *Phys. Rev. B* **1987**, 35, 4031.
- (12) Köhler, W.; Friedrich, J. *Phys. Rev. Lett.* **1987**, 59, 2199.
- (13) Köhler, W.; Friedrich, J.; Scheer, H. *Phys. Rev. A* **1988**, 37, 660.
- (14) Köhler, W.; Zollfrank, J.; Friedrich, J. *Phys. Rev. B* **1989**, 39, 5414.
- (15) Zollfrank, J.; Friedrich, J. *J. Chem. Phys.* **1990**, 93, 8586.
- (16) Schellenberg, P.; Friedrich, J.; Daltrozzo, E. *J. Chem. Phys.* **1991**, 95, 189.
- (17) Kasha, M.; Rawls, H. R.; El-Bayoumi, M. A. *Pure Appl. Chem.* **1965**, 11, 371.